A new finite-difference time-domain method for photonic crystals consisting of nearly-free-electron metals



2001 J. Phys. A: Math. Gen. 34 9713

(http://iopscience.iop.org/0305-4470/34/45/310)

INSTITUTE OF PHYSICS PUBLISHING JOURNAL OF PHYSICS A: MATHEMATICAL AND GENERAL

J. Phys. A: Math. Gen. **34** (2001) 9713–9721 PII: S0305-4470(01)26701-8

# A new finite-difference time-domain method for photonic crystals consisting of nearly-free-electron metals

**Sailing He[1,2], Sanshui Xiao[1], Linfang Shen[1], Jiangping He[1] and Jian Fu[1]**

[1] Centre for Optical and Electromagnetic Research, State Key Laboratory for Modern Optical Instrumentation, Zhejiang University, Yu-Quan, Hangzhou 310027, People's Republic of China
[2] Department of Electromagnetic Theory, Royal Institute of Technology, S-100 44 Stockholm, Sweden

Received 10 July 2001, in final form 17 September 2001
Published 2 November 2001
Online at stacks.iop.org/JPhysA/34/9713

**Abstract**

A finite-difference time-domain method is developed to treat a nearly-free-electron metal by rewriting the time-domain Maxwell's equations into three coupled partial differential equations for three vector functions. The method is used to calculate the band structures of two-dimensional metallic photonic crystals, and the numerical results are compared with those obtained by other methods. The new time-stepping formulae are also used to investigate the defect modes by calculating the transmission spectrum.

PACS numbers: 42.70.Qs, 02.70.Bf, 78.20.Bh

## 1. Introduction

A photonic crystal is a periodic arrangement of dielectric or metallic materials. Photonic crystals have recently attracted wide attention in both physics and engineering communities [1–4] due to the possibility of eliminating electromagnetic wave propagation within a frequency band (a photonic bandgap). Most of the potential applications of photonic crystals rely on the band structure of the dispersion curves.

As we have noted, most theoretical and experimental studies of two-dimensional photonic band structures have been carried out for dielectric systems whose components are characterized by dielectric constants that are real, positive, and frequency independent. It is of interest to explore the consequences for photonic band structures including components characterized not by purely dielectric constants, but dielectric functions that are frequency dependent and can be negative in some frequency range. In recent years, a variety of methods, such as the plane-wave expansion method [5–8], multiple-scattering theory (Korringa–Kohn–Rostoker method) [9–14], transfer matrix method [15–18], finite-difference method [19–26], etc, have been used to calculate the photonic band structures for both *dielectric* and *metallic*

  

photonic crystals. In this paper, we present a new finite-difference time-domain (FDTD) method for calculating the band structures of photonic crystals consisting of nearly-free-electron metals. Compared to the methods mentioned previously, our method is an order-$N$ method for treating a metal characterized by a Drude-like relative dielectric function (a plane-wave expansion method is of the order $N^3$) and the electromagnetic fields are calculated in the time domain.

When the frequency of the electromagnetic wave is low (much lower than the collision frequency of the electrons in the metal), a metal can be described by a frequency-independent conductivity (or, an equivalent complex relative permittivity $\varepsilon_r(\omega) = 1 + \mathrm{i}\sigma/\omega$ (for $\mathrm{e}^{-\mathrm{i}\omega t}$ time dependence), whose imaginary part is proportional to $\omega^{-1}$). For such a case, one can calculate the band structure by, for example, a perturbative plane-wave approach [8] or a conventional FDTD method [25].

In this paper, we consider the high-frequency case when the frequency of the light is much higher than the collision frequency of the electrons in the metal. For such a case, the nearly-free-electron metal can be described by the following frequency-dependent relative permittivity (see, for example, [27])

$$\varepsilon_r(\omega) = 1 - \frac{\omega_\mathrm{p}^2}{\omega^2} \tag{1}$$

where $\omega_\mathrm{p}$ is the plasma frequency of the conduction electrons. Note that the above equivalent permittivity has a real value and is positive when $\omega > \omega_\mathrm{p}$ but negative when $\omega < \omega_\mathrm{p}$. For such a case, a modified plane-wave expansion method has been applied after transforming Maxwell's equations into an eigenvalue system with some manipulation [7]. However, such a plane-wave expansion method is of the order $N^3$ (i.e., the computational time grows at a rate of $N^3$ as $N$—the number of expansion terms or discretization points in a cell—increases). As one of the major advantages, the present method is of the order $N$. In common with earlier work [23], equation (1) is based on a plasmon pole approximation to the dielectric function. In our method, the variables have a more physical interpretation than those of [23]. We modify the FDTD method to treat the nearly-free-electron metal and use it to calculate the band structure of two-dimensional metallic photonic crystals. The method is also used to investigate defect modes by calculating the transmission spectrum (as a scattering problem [28]; note that the plane-wave expansion method is not applicable to a scattering problem).

## 2. Theory and the new time-stepping formulae

In this section we rewrite Maxwell's equations for a nearly-free-electron metal and introduce new time-stepping formulae in a FDTD approach.

We start with Maxwell's equations

$$\begin{aligned} \nabla \times \boldsymbol{E} &= -\frac{\partial \boldsymbol{B}}{\partial t} \\ \nabla \times \boldsymbol{H} &= \frac{\partial \boldsymbol{D}}{\partial t}. \end{aligned} \tag{2}$$

In the frequency domain, the electric displacement $\boldsymbol{D}(\omega) = \varepsilon_0 \varepsilon_r(\omega)\boldsymbol{E}(\omega)$. In a time-domain treatment, a frequency-dependent permittivity $\varepsilon_r(\omega)$ (cf equation (1)) gives rise to a time convolution with a dispersion kernel in the time-domain constitutive relation $\boldsymbol{D} = \varepsilon_0\big[\boldsymbol{E} + \int_0^t \chi(t - t')\boldsymbol{E}(t')\,\mathrm{d}t'\big]$, where $\chi(t)$ is called the susceptibility kernel [27]. Such a time convolution consumes much computational time and memory in a FDTD approach (note that one needs to save the field data at all the earlier times in order to evaluate the convolution). In this paper, we avoid such a time convolution by introducing a third function and

rewriting Maxwell's equations as a set of partial differential equations (PDEs) with *frequency-independent* coefficients.

From equation (1), one can see that the polarization vector is related to the electric field by the following formula (note that $\boldsymbol{D} = \boldsymbol{P} + \varepsilon_0 \boldsymbol{E}$)

$$\boldsymbol{P} = \varepsilon_0(\varepsilon_r - 1)\boldsymbol{E} = -\varepsilon_0 \frac{\omega_{\mathrm{p}}^2}{\omega^2}\boldsymbol{E}.$$

We denote the time derivative of $\boldsymbol{P}$ as a new function $\boldsymbol{P}_t$, i.e.

$$\frac{\partial \boldsymbol{P}}{\partial t} \equiv \boldsymbol{P}_t.$$

Then we can rewrite Maxwell's equations for a nearly-free-electron metal as the following set of PDEs for the three functions $\boldsymbol{E}$, $\boldsymbol{H}$ and $\boldsymbol{P}_t$

$$\begin{aligned} \frac{\partial \boldsymbol{H}}{\partial t} &= -\frac{1}{\mu_0}\nabla \times \boldsymbol{E} \\ \frac{\partial \boldsymbol{E}}{\partial t} &= \frac{1}{\varepsilon_0}[\nabla \times \boldsymbol{H} - \boldsymbol{P}_t] \\ \frac{\partial \boldsymbol{P}_t}{\partial t} &= \varepsilon_0 \omega_{\mathrm{p}}^2 \boldsymbol{E}. \end{aligned} \tag{3}$$

Note that all the coefficients in the above three PDEs are frequency-independent (i.e., no time convolution is involved). Since the time derivatives of all three functions are given in the above three PDEs, we can find appropriate time-stepping formulae by a time-domain finite difference.

In a two-dimensional case, the fields can be simply decoupled into two transversely polarized modes, namely the $E$-polarization and the $H$-polarization [29]. The corresponding PDEs can be discretized in space and time by a so-called Yee-cell technique [30]. We discretize the entire plane with a mesh of uniform cells formed by lines of constant $x$ and $y$, and obtain a two-dimensional orthogonal mesh. Each discretization cell has lengths $\Delta x$ and $\Delta y$ along the $x$ and $y$ directions, respectively. In the discretized space we denote each grid point by

$$(i, j) = (i\Delta x, j\Delta y) \tag{4}$$

where both $i$ and $j$ are integers. The time $t$ is also discretized with the time increment $\Delta t$, and we denote any function $u$ of space and time evaluated at a grid point and at a discrete time by

$$u|_{i,j}^{n} = u(i\Delta x, j\Delta y, n\Delta t) \tag{5}$$

where $n$ is also an integer. In the discretization of the time variable in equation (3), there is a $\frac{1}{2}\Delta t$ time shift between the magnetic and electric fields and between the electric field and the function $\boldsymbol{P}_t$. For the $E$-polarization, one can express $H_x|_{i,j+\frac{1}{2}}^{n+\frac{1}{2}}$, $H_y|_{i+\frac{1}{2},j}^{n+\frac{1}{2}}$, $E_z|_{i,j}^{n+1}$ and $P_{tz}|_{i,j}^{n+\frac{1}{2}}$ in terms of their values at a previous time as follows:

$$H_x|_{i,j+\frac{1}{2}}^{n+\frac{1}{2}} = H_x|_{i,j+\frac{1}{2}}^{n-\frac{1}{2}} - \frac{\Delta t}{\mu_0}\left[\frac{E_z|_{i,j+1}^{n} - E_z|_{i,j}^{n}}{\Delta y}\right] \tag{6}$$

$$H_y|_{i+\frac{1}{2},j}^{n+\frac{1}{2}} = H_y|_{i+\frac{1}{2},j}^{n-\frac{1}{2}} + \frac{\Delta t}{\mu_0}\left[\frac{E_z|_{i+1,j}^{n} - E_z|_{i,j}^{n}}{\Delta x}\right] \tag{7}$$

$$E_z|_{i,j}^{n+1} = E_z|_{i,j}^{n} - \frac{\Delta t}{\varepsilon_0}P_{tz}|_{i,j}^{n+\frac{1}{2}} + \frac{\Delta t}{\varepsilon_0}\left[\frac{H_y|_{i+\frac{1}{2},j}^{n+\frac{1}{2}} - H_y|_{i-\frac{1}{2},j}^{n+\frac{1}{2}}}{\Delta x} - \frac{H_x|_{i,j+\frac{1}{2}}^{n+\frac{1}{2}} - H_x|_{i,j-\frac{1}{2}}^{n+\frac{1}{2}}}{\Delta y}\right] \tag{8}$$

$$P_{tz}|_{i,j}^{n+\frac{1}{2}} = P_{tz}|_{i,j}^{n-\frac{1}{2}} + \Delta t\varepsilon_0\omega_{\mathrm{p}}^2|_{i,j}E_z|_{i,j}^{n}. \tag{9}$$

In a similar manner, we can obtain the following time-stepping formulae for the $H$-polarization case:

$$H_z|_{i,j}^{n+1} = H_z|_{i,j}^{n} - \frac{\Delta t}{\mu_0}\left[\frac{E_y|_{i+\frac{1}{2},j}^{n+\frac{1}{2}} - E_y|_{i-\frac{1}{2},j}^{n+\frac{1}{2}}}{\Delta x} - \frac{E_x|_{i,j+\frac{1}{2}}^{n+\frac{1}{2}} - E_x|_{i,j-\frac{1}{2}}^{n+\frac{1}{2}}}{\Delta y}\right] \tag{10}$$

$$E_x|_{i,j+\frac{1}{2}}^{n+\frac{1}{2}} = E_x|_{i,j+\frac{1}{2}}^{n-\frac{1}{2}} - \frac{\Delta t}{\varepsilon_0} P_{tx}|_{i,j+\frac{1}{2}}^{n} + \frac{\Delta t}{\varepsilon_0}\left[\frac{H_z|_{i,j+1}^{n} - H_z|_{i,j}^{n}}{\Delta y}\right] \tag{11}$$

$$E_y|_{i+\frac{1}{2},j}^{n+\frac{1}{2}} = E_y|_{i+\frac{1}{2},j}^{n-\frac{1}{2}} - \frac{\Delta t}{\varepsilon_0} P_{ty}|_{i+\frac{1}{2},j}^{n} - \frac{\Delta t}{\varepsilon_0}\left[\frac{H_z|_{i+1,j}^{n} - H_z|_{i,j}^{n}}{\Delta x}\right] \tag{12}$$

$$P_{tx}|_{i,j+\frac{1}{2}}^{n+1} = P_{tx}|_{i,j+\frac{1}{2}}^{n} + \Delta t \varepsilon_0 \omega_{\mathrm{p}}^2|_{i,j+\frac{1}{2}} E_x|_{i,j+\frac{1}{2}}^{n+\frac{1}{2}} \tag{13}$$

$$P_{ty}|_{i+\frac{1}{2},j}^{n+1} = P_{ty}|_{i+\frac{1}{2},j}^{n} + \Delta t \varepsilon_0 \omega_{\mathrm{p}}^2|_{i+\frac{1}{2},j} E_y|_{i+\frac{1}{2},j}^{n+\frac{1}{2}}. \tag{14}$$

In all these time-stepping formulae, we set $\omega_{\mathrm{p}}|_{i,j} = 0$ when the point $(i, j)$ is in vacuum. If one knows all the necessary information at each grid point, such as the plasma frequency $\omega_{\mathrm{p}}$ and the initial distribution of the fields, one can obtain the time evolution of the fields by these time-stepping formulae. From these time-stepping formulae, one can easily see that for a fixed total number of time steps the computational time is proportional to the number of discretization points in the computation domain, i.e. the present algorithm is of the order $N$ (note that the plane-wave expansion method is of the order $N^3$).

## 3. Numerical results and discussions

In this section, we use the time-stepping formulae (6)–(14) to calculate the band structure of two-dimensional metallic photonic crystals, as well as to investigate defect modes by calculating the transmission spectrum. In all our FDTD numerical results presented in this paper we choose $\Delta t = 1/\left(10c\sqrt{\Delta x^{-2} + \Delta y^{-2}}\right)$, where $c$ is the speed of light in vacuum.

### *3.1. Photonic band structures*

Since the photonic crystal is a periodic structure, one naturally chooses a unit cell of a lattice as the finite computation domain. When calculating the fields at the boundary of the computation domain (a unit cell of a lattice), the time-stepping formulae require the field values at the space point $(i\Delta x, j\Delta y)$ which is out of the computation domain. We use the periodic boundary condition to obtain this required field value $u(i\Delta x, j\Delta y)$ through the known field value at the corresponding position inside the computation domain. In this paper, we use a pseudo-periodic field distribution as the initial field at time $t = 0$ (see, for example, [25]). The dispersion relation (i.e. the band structure) of the metallic photonic crystal is a relation between the frequency $\omega$ and the wave vector $\boldsymbol{k}$. After all the fields are obtained in the time domain, we transform the calculated fields from the time domain to the frequency domain by a Fourier transform and the peaks of the spectral distribution correspond to the locations of the *eigen* frequencies [25].

In order to verify the present approach, we compare the band structures obtained by our formulae with those computed by other methods.

Firstly, we compare our results with those obtained by the order-$N$ approximation method described in [23]. We calculate the photonic band structure of a square lattice of parallel metal rods of a square cross section, embedded in vacuum. We choose $\omega_{\mathrm{p}} a/(2\pi c) = 1$ ($a$ is the lattice constant), and the metal filling fraction $f = 0.01$. The unit lattice cell contains $100 \times 100$ grid

points, and the total number of time steps is 20 000. The band structures for the $E$-polarization and the $H$-polarization are shown in figures 1($a$) and ($b$), respectively. The circles are obtained by our method and the solid curves are obtained by the approximation method of [23]. As one can see from these figures, our results give a good agreement with the results obtained by the method of [23]. One of the reasons for the small discrepancy is that the method in [23] is an approximate method (the frequency-dependent permittivity is approximated by an expansion as a series of poles). The dotted curves in figures 1($a$) and ($b$) indicate the corresponding band structure for the homogeneous background medium (i.e. when there are no metallic inclusions). One can clearly see from figure 1($a$) that the metallic inclusions lift the first band of the $E$-polarization and cause a stop band at the lowest frequencies. The cut-off is due to the collective motion of electrons (of the metal) in the electric field parallel to the rods below some effective plasma frequency associated with a specific filling fraction (see, for example, [23]). Unlike the case of $E$-polarization, the photonic band structures for the $H$-polarization possess a number of quite flat (nearly non-dispersive) bands (the left parts of the second and third bands and the right part of the fourth band in figure 1($b$)) in the frequency range $\omega < \omega_p$, effectively superimposed on the dispersive band structure. This is quite different from the band structure for the homogeneous background medium. These flat bands are caused by the resonant modes of the individual rods, which are excited by the electric field perpendicular to the rods (see, for example, [23]; note that in the $E$-polarization the electric field is parallel to the rods and thus such flat bands do not exist in the case of $E$-polarization).

Next we compare our results with those obtained by a modified plane-wave expansion method presented in [7]. We calculate the photonic band structure of a square lattice of metal cylinders (with $\omega_p a/(2\pi c) = 1$) in vacuum for the $E$-polarization (we do not present the corresponding results for the $H$-polarization since it is difficult to find a bandgap for the case of $H$-polarization and we wish to find defect modes within a bandgap in the next subsection). A bandgap starts to appear when the filling fraction $f \geqslant 0.25$, and it increases as the filling fraction increases until it reaches a maximal bandgap at $f = 0.7$ (see figures 2($a$) and ($b$) of [7]). Therefore, we choose the metal filling fraction $f = 0.7$ (i.e. the radius of the metallic cylinder $R = 0.472a$) in this example. In figure 2, the circles are obtained by our method and the solid curves are obtained by the modified plane-wave method [7]. From this figure, one can see that our results are consistent with those obtained by the modified plane-wave method [7]. One can also see that for this polarization there is a photonic bandgap (indicated by the shaded region), which will be used below to study defect modes inside this bandgap. Compared to the modified plane-wave expansion method, the present time-stepping method is of the order $N$ (the modified plane-wave expansion method is of the order $N^3$) and can treat a scattering problem (as shown below; the plane-wave expansion method is not applicable to a scattering problem).

### *3.2. The transmission spectrum method for defect modes*

The present time-stepping formulae can also be used to investigate defect modes in a metallic photonic crystal by calculating the transmission spectrum in a scattering set-up.

We consider a finite-sized $21 \times 7$ photonic crystal (the same metallic photonic crystal as used for figure 2) in which a point defect has been introduced by changing the radius of a metal rod in one unit cell. Plane waves are sent at normal incidence, and the transmission through the photonic crystal is computed. The set-up is shown in figure 3. Each unit cell contains 1681 ($41 \times 41$) discretization grid points for the time-stepping formulae. The computation domain is surrounded by a perfectly matched layer (PML; see, for example, [31]) with 12 layers of the discretization grid. The total number of time steps is 30 000. The transmission spectra

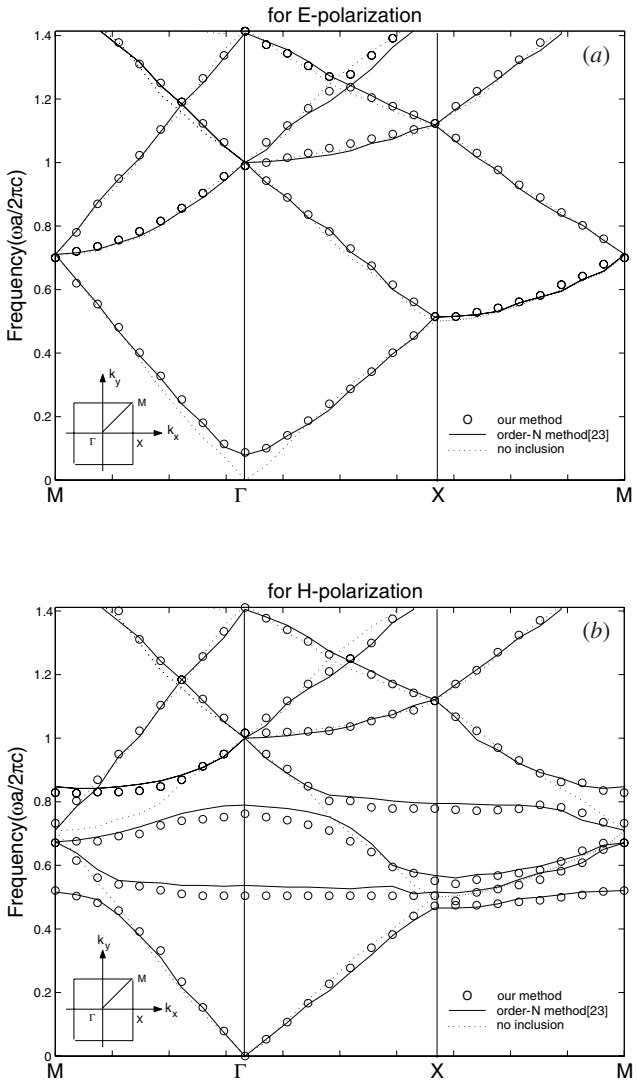


**Figure 1.** Photonic band structure for a square lattice of metal rods with a square cross section. The filling fraction $f = 0.01$, and $\omega_p a/(2\pi c) = 1$. The circles are obtained by our method, and the solid curves are obtained by the approximation method of [23]. The dashed curves give the corresponding band structure for the homogeneous background medium (i.e. there is no inclusion). (*a*) For the $E$-polarization; (*b*) for the $H$-polarization.

through the photonic crystal are calculated at a single point marked 'detector' in figure 3. A pulse which has a Gaussian spectrum centred at the frequency 0.7 ($2\pi c/a$) is impinged on the photonic crystal. The spectrum of the incident pulse is shown in figure 4. The transmission spectra (normalized with respect to the incident amplitude) are shown in figure 5. The solid curve and the dotted curve correspond to the case without defect (i.e. $R_d = 0.472a$) and the case with a defect ($R_d = 0.2a$), respectively. The solid curve in figure 5 indicates that there are two stop bands for the $E$-polarization for such a metallic photonic crystal and the locations of these two stop bands are consistent with the two bandgaps in figure 2. Note that the two stop bands of the solid curve in figure 5 are larger than the two bandgaps indicated in figure 2.

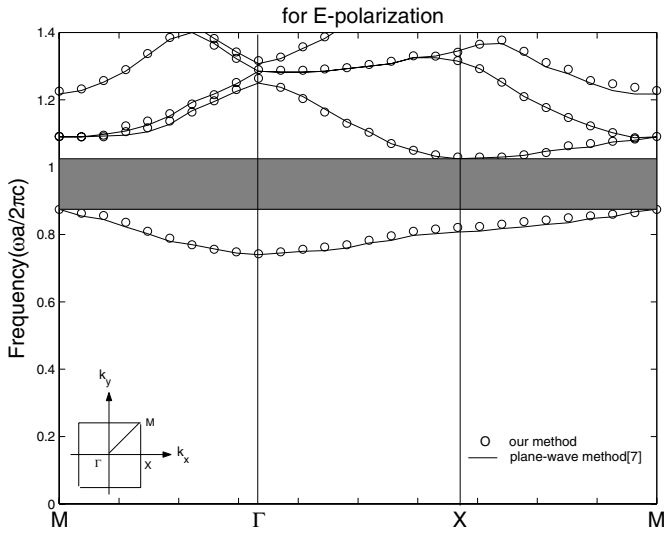


**Figure 2.** Photonic band structure for a square lattice of metallic cylinders in vacuum. The filling fraction $f = 0.7$ (corresponding to $R = 0.472a$), and $\omega_p a/(2\pi c) = 1$. The circles are obtained by our method, and the solid curves are obtained by a modified plane-wave expansion method [7].

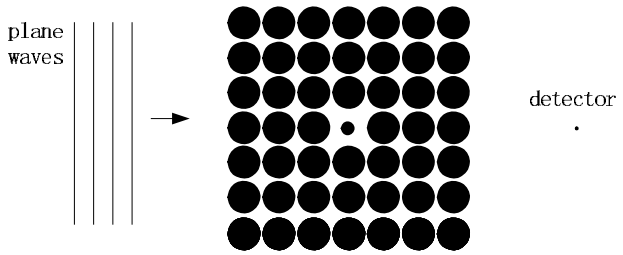


**Figure 3.** Set-up for the computation of the transmission spectrum.

This is because the two bandgaps in figure 2 are for all incident directions while the stop bands in figure 5 are only for propagation along the normal direction ($k_y = 0$). From figures 2 and 5, we can also see that the position of the gaps in the transmission spectrum, which is obtained for plane electromagnetic waves incident normally ($k_y = 0$) on a finite slab of the photonic crystal without defect, agrees very well with the position of the gaps in the frequency band structure of the corresponding infinite crystal along the $\Gamma$–$X$ direction ($k_y = 0$).

Modes outside the gap can be transmitted efficiently (some frequencies have a transmission coefficient close to unity). On the other hand, modes inside the bandgap are strongly attenuated. They cannot propagate through the crystal and are reflected back. When a defect is introduced by changing the radius $R_d$ of a metal rod in the photonic crystal, the simulation result (the dotted curve in figure 5) shows the presence of three sharp resonances inside the second gap. Our method gives three eigenfrequencies, namely, $\omega_d = 0.931$, 0.987 and 1.005 ($2\pi c/a$) for the defect with $R_d = 0.2a$. At these resonant frequencies, a certain amount of energy of the electromagnetic waves can go through the finite-sized photonic crystal even though these resonant frequencies are inside the bandgap of the corresponding perfect photonic crystal. The electric field distributions of the defect modes for the defect in the corresponding perfect photonic crystal can be calculated in a way similar to [26].

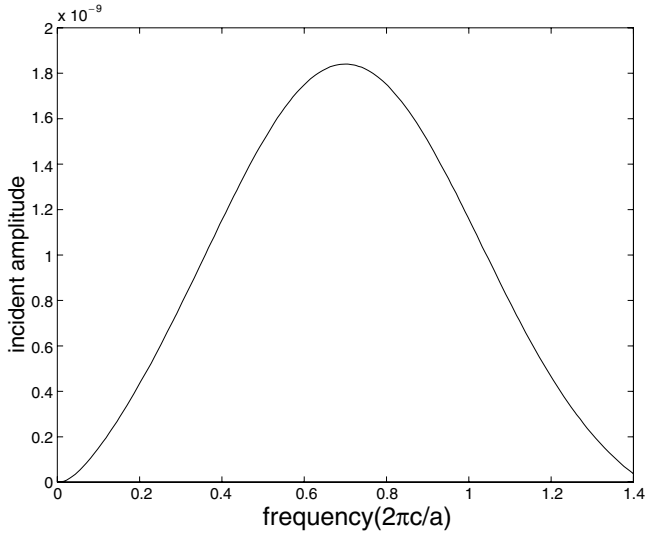


**Figure 4.** Gaussian spectrum of the incident pulse.

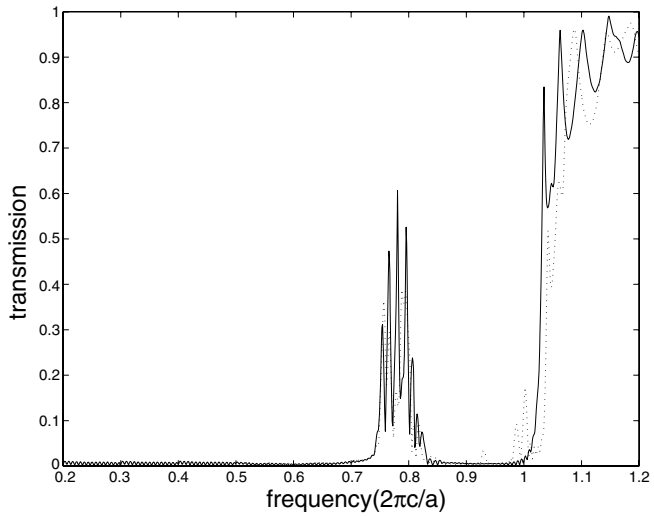


**Figure 5.** Normalized transmission through a finite-sized 21 × 7 metallic photonic crystal (the same metallic photonic crystal as used for figure 2) as the frequency varies. The solid curve is for the case when there is no defect. The dotted curve is for the case when the radius of the defect rod is $R_{\mathrm{d}} = 0.2a$.

## 4. Conclusion

We have modified the FDTD method to treat a nearly-free-electron metal. The time-domain Maxwell's equations have been rewritten into three coupled PDEs (without time convolution) for three vector functions. The method has been used to calculate the band structure of two-dimensional metallic photonic crystals, and the results have been compared with those obtained by other methods, namely, an order-$N$ approximation method and a modified plane-

wave expansion method (which is of the order $N^3$). The new time-stepping formulae have also been used to obtain the eigenfrequencies of the defect modes by calculating the transmission spectrum.

## Acknowledgment

The partial support of the Division of Science and Technologies of Zhejiang provincial government (ZD0002) under a key project grant is gratefully acknowledged.

## References

[1] Yablonovitch E 1987 *Phys. Rev. Lett.* **58** 2059
[2] Joannopoulos J D, Villeneuve P R and Fan S 1997 *Nature* **386** 143
[3] Joannopoulos J D, Meade R D and Winn J N 1995 *Photonic Crystals: Molding the Flow of Light* (Princeton, NJ: Princeton University Press)
[4] C M Soukoulis (ed) 1993 *Photonic Band Gaps and Localization, Proc. NATO ARW* (New York: Plenum)
[5] Ho K M, Chan C T and Soukoulis C M 1990 *Phys. Rev. Lett.* **65** 3152
[6] Zhang Z and Satpathy S 1990 *Phys. Rev. Lett.* **65** 2650
[7] Kuzmiak V, Maradudin A A and Pincemin F 1994 *Phys. Rev.* B **50** 16 835
[8] Kuzmiak V and Maradudin A A 1997 *Phys. Rev.* B **55** 7427
[9] Ohtaka K 1979 *Phys. Rev.* B **19** 5057
[10] Leung K M and Qiu Y 1993 *Phys. Rev.* B **48** 7767
[11] Yannopapas V, Modinos A and Stefanou N 1999 *Phys. Rev.* B **60** 5359
[12] Zhang W Y, Lei X Y, Wang Z L, Zheng D G, Tam W Y, Chan C T and Sheng P 2000 *Phys. Rev. Lett.* **84** 2853
[13] Modinos A, Stefanou N and Yannopapas V 2001 *Opt. Express* **8** 197
[14] Stefanou N, Modinos A and Yannopapas V 2001 *Solid State Commun.* **118** 69
[15] Pendry J B and MacKinnon A 1992 *Phys. Rev. Lett.* **69** 2772
[16] Sigalas M M, Chan C T, Ho K M and Soukoulis C M 1995 *Phys. Rev.* B **52** 11 744
[17] Pendry J B, Holden A J, Stewart W J and Youngs I 1996 *Phys. Rev. Lett.* **76** 4773
[18] Garcia-Vidal F J and Pendry J B 1996 *Phys. Rev. Lett.* **77** 1163
[19] Chan C T, Yu Q L and Ho K M 1995 *Phys. Rev.* B **51** 16 635
[20] Ward A J and Pendry J B 1998 *Phys. Rev.* B **58** 7252
[21] Fan S, Villeneuve P R and Joannopoulos J D 1996 *Phys. Rev.* B **54** 11 245
[22] Sievenpiper D F, Yablonovitch E, Winn J N, Fan S, Villeneuve P R and Joannopoulos J D 1998 *Phys. Rev. Lett.* **80** 2829
[23] Arriaga J, Ward A J and Pendry J B 1999 *Phys. Rev.* B **59** 1874
[24] Sigalas M M, Biswas R, Ho K M, Soukoulis C M and Crouch D D 1999 *Phys. Rev.* B **60** 4426
[25] Qiu M and He S 2000 *J. Appl. Phys.* **87** 8268
[26] Qiu M and He S 2000 *Phys. Rev.* B **61** 12 871
[27] Jackson J D 1975 *Classical Electrodynamics* (New York: Wiley)
[28] Villeneuve P R, Shanhui Fan and Joannopoulos J D 1996 *Phys. Rev.* B **54** 7837
[29] Taflove A 1995 *Computational Electrodynamics: The Finite-Difference Time-Domain Method* (Norwood: Artech House Publishers)
[30] Yee K S 1966 *IEEE Trans. Antennas Propag.* **14** 302
[31] Berenger J P 1994 *J. Comput. Phys.* **114** 185